

How can amorphous silicon improve current gravitational-wave detectors?

Jessica Steinlechner^{1,2,3,*} and Iain W. Martin³¹*Maastricht University, P.O. Box 616, 6200 MD Maastricht, Netherlands*²*Nikhef, Science Park 105, 1098 XG Amsterdam, Netherlands*³*SUPA, School of Physics and Astronomy, University of Glasgow, Glasgow, G12 8QQ, Scotland*

(Received 5 October 2020; accepted 13 January 2021; published 1 February 2021)

Thermal noise in the highly reflective mirror coatings is one of the main limitations to the sensitivity of current gravitational-wave detectors. Amorphous silicon (aSi) is an ideal material to reduce thermal noise. Due to high optical absorption at 1064 nm, so far it was mainly considered as a candidate for future, cryogenic detectors using longer wavelengths. This paper summarizes the current state-of-the-art of the optical absorption of aSi at 1064 nm. We show how recent improvements in aSi absorption, and the development of multimaterial coatings, make the use of aSi at 1064 nm realistic, and discuss the possible thermal-noise improvement and corresponding optical absorption in room-temperature gravitational-wave detectors.

DOI: [10.1103/PhysRevD.103.042001](https://doi.org/10.1103/PhysRevD.103.042001)

I. INTRODUCTION

During their first two observing runs, Advanced LIGO [1] and Advanced Virgo [2] detected several gravitational-wave signals from binary black hole mergers and from a neutron-star merger [3–8]. These gravitational-wave detectors are kilometer-scale Michelson interferometers measuring changes in the separation of suspended, highly reflective coated mirrors. Thermal noise originating from the mirror coatings will limit the performance of the detectors at their most sensitive frequencies once they have reached their design sensitivity. To further increase the sensitivity and therefore the number of detected signals, improved optical coatings are essential.

Currently, Advanced LIGO and Advanced Virgo use coatings made from alternating layers of silica (SiO_2) and tantalum doped with titania ($\text{TiO}_2:\text{Ta}_2\text{O}_5$) [1,2]. The $\text{TiO}_2:\text{Ta}_2\text{O}_5$ (from now on referred to as Ta_2O_5) layers dominate coating thermal noise due to a mechanical loss significantly higher than that of SiO_2 at room temperature [9–13]. Approaches to reduce coating thermal noise include improving Ta_2O_5 by understanding correlations between the atomic structure and material properties [14–16], elevated temperature deposition [17], and different dopants and doping concentrations [11].

Another option is to replace the Ta_2O_5 layers in the coating by an alternative amorphous material. However, in addition to low mechanical loss, the highly reflective coatings are required to show low optical absorption of, ideally, < 1 ppm (10^{-6}) to avoid thermal distortions of the

mirror due to heating. The optical absorption of the best highly reflective coatings made of SiO_2 and Ta_2O_5 is ≈ 0.27 ppm [18]. Several potential alternative coating materials were investigated over the past years [19–23]; however, achieving a significant thermal-noise improvement and simultaneously keeping the optical absorption low is extremely challenging.

A completely different approach under investigation is the use of crystalline coatings, such as AlGaAs [24]. Crystalline coatings show a significant thermal-noise reduction and low optical absorption, but come with other obstacles such as coating-size limitations and the requirement to remove the coatings from the lattice-matched substrate they are grown on and bond them to the final mirror-substrate used in the detector.

Amorphous silicon (aSi) is a candidate coating material with a low mechanical loss [25] of up to 10 times below that of Ta_2O_5 . A high refractive index of 3.5 at 1064 nm makes aSi even more interesting as, due to the high contrast to SiO_2 ($n = 1.45$ [26,27]), fewer layers of both coating materials are required to achieve high reflectivity. This additionally reduces thermal noise, which scales with the coating thickness.

Initially, the optical absorption of aSi was found to be far too high for using it in gravitational-wave detector coatings: at 1064 nm, an extinction coefficient of $k = 7.4 \times 10^{-3}$ was found after optimum heat treatment (corresponding to ≈ 4000 ppm for an highly reflective coating made of aSi and SiO_2 [28]). However, the past few years have shown a significant absorption reduction to $k = 2.0 \times 10^{-4}$ [23]. In this paper, we show that at this level of absorption, the use of aSi at 1064 nm is starting to be realistic—when used in a multimaterial design.

*Jessica.Steinlechner@ligo.org

Multimaterial coating designs have been proposed to enable the use of materials with high optical absorption, but low mechanical loss [29,30]. Low-absorption materials are used for the upper coating layers, which reflect the majority of the incident laser power. Further down in the coating, where the power is low, higher-absorbing materials with low mechanical loss can be used to reduce the overall thermal noise of the coating. Recently, the multimaterial concept has been experimentally verified: for a proof-of-concept coating, it has been shown that the incorporation of layers with low mechanical loss, but rather high optical absorption, can reduce thermal noise, while low-absorbing layers in the upper layers can keep the total absorption low. Furthermore, it has been shown that heat treatment does not cause damages such as cracks to the multimaterial coating [31].

In this paper, we give an overview of the current status of aSi absorption at 1064 nm and room temperature. We discuss how multimaterial designs—in which as many layers of Ta₂O₅ as possible are replaced by aSi—can improve the thermal noise of highly reflective coatings for detectors such as Advanced LIGO, operating at 1064 nm at room temperature. Furthermore, we show that the absorption can additionally be reduced by using some split aSi and Ta₂O₅ layers.

II. HIGHLY REFLECTIVE MIRROR COATINGS

This section gives an introduction to the optical and thermal-noise performance of highly reflective mirror coatings.

A. Optical absorption

The optical absorption of a material is proportional to the *extinction coefficient* k . The extinction coefficient is the imaginary part of the complex refractive index $\mathbf{n} = n + ik$. We will refer to the real part, n , as *refractive index* throughout this paper. Highly reflective mirror coatings are made of stacks of layers with alternating low and high refractive index.

The reflectivity of the coating depends on the refractive-index contrast at the layer interfaces and on the phase within the layers determined by their optical thickness $n \times d$, where d is the geometric thickness. For an optical thickness of $\lambda/4$ (or odd multiples of this value), the light field within the layers minimizes, resulting in maximum reflectivity. A larger n of one of the coating materials decreases d for all the layers made of this material. If it results in a larger refractive-index contrast between the materials, the total number of (pairs of) layers required to achieve the design reflectivity also reduces. As thermal noise is proportional to d , a thin coating is generally desirable; see Sec. II B.

Figure 1 shows a coating stack made of a total of 17 layers of SiO₂ (blue, $n = 1.44$ at 1064 nm) and 18 layers of

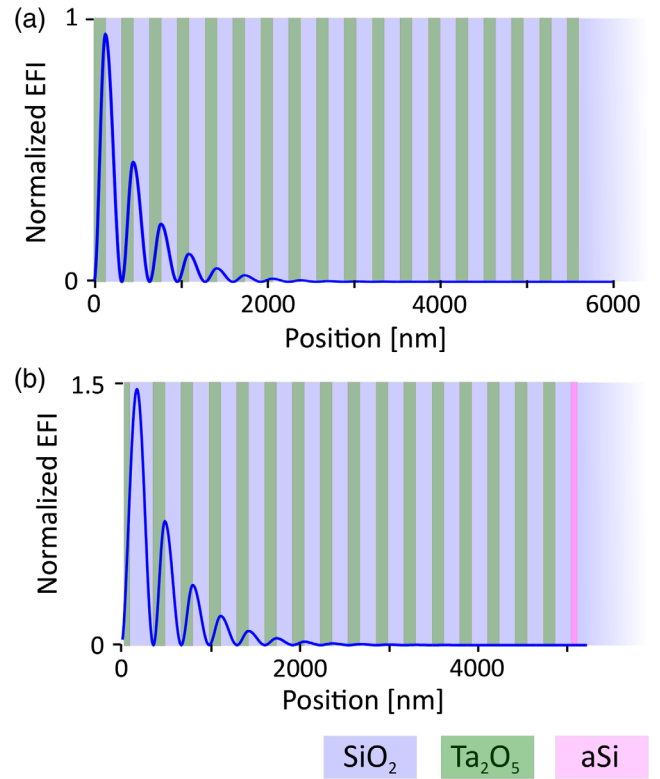


FIG. 1. (a) Schematic of a highly reflective coating stack made of alternating layers of Ta₂O₅ (green, high n) and SiO₂ (blue, low n) on a SiO₂ substrate. The thickness of all layers is $\lambda/4$. The dark-blue line shows the laser light (electric field) intensity (EFI). (b) The Ta₂O₅ layer closest to the substrate was replaced by aSi (pink). The number of Ta₂O₅/SiO₂ layers above was adjusted for coating (b) to have the same reflectivity as (a).

Ta₂O₅ (green, $n = 2.07$ at 1064 nm) on a SiO₂ substrate, resulting in a reflectivity of 99.9994%.¹ The amplitude of the blue line, representing the electric-field (light-field) intensity (EFI) within the coating, decreases with every pair of layers—in the example of SiO₂ and Ta₂O₅ by about 50%. The optical absorption in a coating layer is proportional to the spatial integral of the EFI. Consequently, layers contribute less to the total absorption the further down in the coating they are placed.

B. Coating thermal noise

Coating thermal noise amplitude spectral density—from now on referred to as coating thermal noise (CTN)—is given by [30]

$$x(f) = \sqrt{\frac{2k_B T}{\pi^2 f} \frac{1}{w^2} \frac{1 - \sigma_{\text{sub}} - 2\sigma_{\text{sub}}^2}{Y_{\text{sub}}} \sum_j b_j d_j \phi_j}. \quad (1)$$

¹Note that for the gravitational-wave detectors, the design can differ slightly from this simple case in order to optimize coating parameters, e.g., making it reflective at more than one wavelength.

TABLE I. Material parameters of aSi. More detail about the data can be found in [35]. The errors in k and ϕ are taken to be $< 10\%$ (see main text for further explanation).

Deposition		Measured parameters				Other parameters	
Facility	Method	T [°C]	ϕ	k	n	Y [GPa]	σ
MLD	IBS	600	9×10^{-5} ^a	1.1×10^{-2}	3.34 ± 0.06	147 [36]	0.23
ATF	IBS	450	9×10^{-5} [37]	9.0×10^{-3} [28]	3.72 ± 0.12
TM	ion plating	500	2×10^{-5} [38]	4.3×10^{-3}	3.82 ± 0.07
UWS	ECR-IBS	400	2×10^{-5} [23]	$2(5) \times 10^{-4}$ [23]	3.39 ± 0.07

^aThe loss was not measured for MLD coatings. For calculations, the loss of ATF coatings was used.

Here, k_B is the Boltzmann constant, T the mirror temperature, f the frequency, and w the radius of the laser beam on the coating. Y_{sub} and σ_{sub} are the Young's modulus and the Poisson ratio of the mirror substrate. d and ϕ are the coating thickness and the mechanical loss with the index j referring to the j th layer in the coating (starting from the outermost layer). We assume here that the mechanical losses associated with bulk motion and shear motion [32] are approximately equal ($\phi_{\text{bulk}} \approx \phi_{\text{shear}} \approx \phi$).

In a first approximation, CTN reduces with the square root of the coating thickness [33]. However, the weighting factor b_j for each coating layer described by

$$b_j = \frac{(1 - 2\sigma_j)(1 + \sigma_j)}{(1 - 2\sigma_{\text{sub}})(1 + \sigma_{\text{sub}})} \frac{1}{1 - \sigma_j} \times \left[\left(1 - n_j \frac{\partial \theta_{\text{coat}}}{\partial \theta_j} \right)^2 \frac{Y_{\text{sub}}}{Y_j} + \frac{(1 - \sigma_{\text{sub}} - 2\sigma_{\text{sub}}^2)^2}{(1 + \sigma_j)^2 (1 - 2\sigma_j)} \frac{Y_j}{Y_{\text{sub}}} \right], \quad (2)$$

where n_j is the refractive index of the j th layer, shows that the lower coating layers contribute more to the total CTN than the upper layers. The first term in the square brackets of Eq. (2) describes thermal noise arising from fluctuations in coating thickness. It is composed of two effects: a fluctuation in a layer changing (1) the optical thickness of this layer, and (2) the position of the front surface of the mirror. These two effects work in opposite directions and partly compensate. The first effect leads to fluctuations in the round-trip phase in each layer, θ_j . The sensitivity of the total coating phase, θ_{coat} , to these fluctuations, is described by $\partial \theta_{\text{coat}} / \partial \theta_j$. The magnitude of the latter is proportional to the peak EFI in the j th layer. As explained in Sec. II A, the EFI reduces with each double layer resulting in the first effect being smaller for layers positioned further down in the coating, while the second effect is independent of the layer position. Therefore, in lower layers, the first effect compensates less for the second effect so that these layers contribute more strongly to b_j and consequently, to the overall CTN.

III. AMORPHOUS SILICON ABSORPTION

Future, cryogenic gravitational-wave detectors are likely to use crystalline-silicon mirror substrates and to operate at

longer laser wavelengths at which crystalline silicon is transparent [34]. Therefore, to date, most work on aSi has been targeted at coatings for use at 1550 nm and 2000 nm, where it shows an absorption significantly lower than at 1064 nm. Following the success of this work in reducing the absorption, it is of interest to reconsider the use of aSi at 1064 nm.

The absorption of aSi films tends to reduce with heat treatment, with a minimum occurring at around 500°C,² after which the absorption increases again. Previous measurements on optimally heat-treated, commercially available, ion-beam sputtered (IBS) aSi films showed that, at 1064 nm, k can be as high as $\approx 1 \times 10^{-2}$. aSi deposited by ion plating can have a significantly lower k , of $\approx 4 \times 10^{-3}$. An electron cyclotron resonance (ECR) IBS method has recently been shown to produce aSi films with even lower k —as low as $\approx 2 \times 10^{-4}$ at 1064 nm. These numbers are summarized in Table I.

The lowest absorption in Table I is still far above the level required for a traditional two-material coating as shown in Fig. 1(a). However, it is low enough to allow the use of some aSi instead of Ta₂O₅ in the lower layers of a multimaterial coating—see Fig. 1(b).

In the next section, we will look into replacing some of the lower Ta₂O₅ layers (starting from the layer closest to the substrate, see Fig. 1) and investigate the resulting trade-off between optical-absorption increase and thermal-noise reduction.

IV. MULTIMATERIAL COATING DESIGN: TRADE-OFFS

In this section, we discuss the thermal-noise improvement possible by using aSi in multimaterial designs. In Sec. IV A, we introduce the principle we use for our calculations, in Sec. IV B, we introduce different types of aSi, and in Sec. IV C, we discuss the improvement possible.

A. The principle

The basic principle of the multimaterial approach is to replace Ta₂O₅ layers in the lower part of the coating stack

²The exact temperature of the minimum is found to vary with the deposition method and facility used.

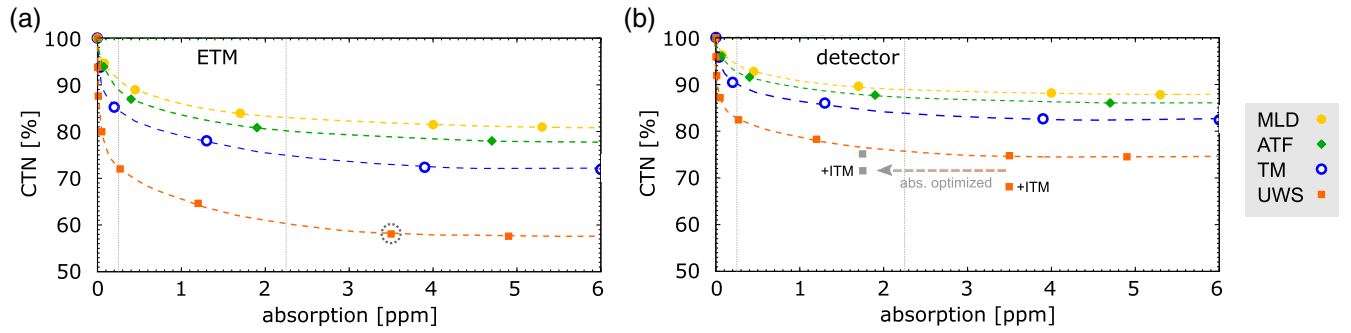


FIG. 2. (a) Relative coating thermal noise of a highly reflective ETM mirror as a function of additional absorption originating from aSi layers for the four different types of aSi discussed. The 100% mark represents a highly reflective $\text{SiO}_2/\text{Ta}_2\text{O}_5$ coating without any aSi, as shown in Fig. 1(a). Each point along the x axis represents one Ta_2O_5 layer at the bottom replaced by one aSi layer. The number of remaining $\text{SiO}_2/\text{Ta}_2\text{O}_5$ was adjusted to keep the reflectivity at 99.9994%. A schematic of the coating represented by the point surrounded by the dotted circle is shown in Fig. 3(a). (b) Coating thermal noise of the whole detector taking into account that in the ITM mirror coatings no Ta_2O_5 can be replaced by aSi. The UWS material is an exception with the additional lower orange point showing the improvement possible when also adding aSi to the ITM. A beam radius of 6.2 cm was assumed for the ETM, while for the ITM a smaller beam radius of 5.5 cm was used—as is the case in Advanced LIGO. The vertical, dotted lines indicate the additional tolerable absorption (left lines: current limit, right lines: potential maximum).

with aSi. This reduces coating thermal noise while the absorption increase is relatively low due to the low laser power at this position.

Figure 1 shows an example: We replace the lowest Ta_2O_5 layer in Fig. 1(a) by aSi (with properties for ATF, see Table I). The aSi layer has a lower loss than Ta_2O_5 , and it is thinner due to the higher refractive index, both directly reducing CTN. The higher n also results in a reflectivity increase from 99.9994% to 99.9998%. To maintain the reflectivity of (a), we remove layers at the top: one complete $\text{SiO}_2/\text{Ta}_2\text{O}_5$ bilayer, plus parts of another bilayer. In this second bilayer, we depart from the $\lambda/4$ design by reducing the thickness of the more lossy Ta_2O_5 to 0.4 quarters, and increasing the low-loss SiO_2 to 1.6 quarters, of a wavelength, so that we maintain a total optical thickness of $\lambda/2$ —as otherwise the center wavelength, at which our coating is reflective, would change. This coating is shown in Fig. 1(b). By replacing one layer of Ta_2O_5 by aSi and “losing” another 1.6 layers, we reduce coating thermal noise by 6% compared to the coating shown in (a). The EFI in the aSi layer at the very bottom of the coating is so low, that the total coating absorption increases by only 0.07 ppm.

The number of Ta_2O_5 layers which can be replaced depends on the tolerable absorption of the final multi-material coating: there is a trade-off between the possible thermal-noise reduction (thermal noise minimizes when all Ta_2O_5 layers are replaced by aSi) and the resulting absorption (which minimizes when no Ta_2O_5 layers are replaced). The thermal-compensation system of Advanced LIGO is designed for 0.5 ppm absorption per coating at maximum laser power [39]. As current coatings absorb 0.27 ppm for the ETMs and 0.22 ppm for the ITMs [40], an additional absorption of ≈ 0.25 ppm should be tolerable without changes. The tolerable absorption may be up to

2.5 ppm with an adjusted compensation system [23,39], allowing for an additional 2.25 ppm of absorption. These absorption levels are indicated by the vertical, dashed lines in Fig. 2. As possible changes to the system have many implications, in this paper, we analyze the possible thermal noise and absorption performance in a number of cases to point out possibilities for consideration.

B. The materials

We consider four different types of aSi coating material for our evaluation of possible thermal-noise improvement:

- (i) two commercially available ion-beam sputtered coatings produced by MLD and ATF,
- (ii) a commercially available ion-plating coating produced by Tafelmaier,
- (iii) and a coating produced in a research lab using a novel type of ECR ion-beam sputtering.

The first two materials are “standard” state-of-the-art aSi, which could be produced in similar quality for use in gravitational-wave detectors without requiring major technological or scientific developments—apart from up-scaling to large sizes, an issue all new materials have in common. These two commercial IBS coatings have higher mechanical loss and optical absorption than the other two coatings.

The Tafelmaier (TM) coatings were produced by ion plating³ and in the past, have consistently shown lower mechanical loss and lower optical absorption than the IBS coatings produced by MLD and ATF. This interesting fact shows us that lower loss and absorption could become

³This technique is unlikely to be used for gravitational-wave detector coatings on short timescales, as it would require several material parameters to be characterized and the development of coating chambers of the required size.

“standard” and could give us some hints of how to modify other coating procedures such as ion-beam sputtering in order to improve aSi.

The ECR-IBS aSi coatings show an order of magnitude lower absorption than the ion-plating coatings, but this deposition procedure is still in the developmental phase and strong variations in properties have been observed [23]. A high-quality, high-uniformity, multilayer optical coating produced using this technique has yet to be demonstrated.

The properties of these four aSi coatings used for our calculations are summarized in Table I [35]. In the following section, we evaluate how much coating thermal noise in gravitational-wave detectors could be improved by using aSi. We discuss all four materials to show the improvement possible without significant further development, but also the possibilities the best aSi demonstrated so far would offer.

C. The improvement

Figure 2(a) shows the possible coating thermal noise for the four types of aSi introduced in the previous section, as a function of the additional absorption originating from the aSi layers. The 100% mark represents a highly reflective $\text{SiO}_2/\text{Ta}_2\text{O}_5$ coating without any aSi, as shown in Fig. 1(a), with a reflectivity of 99.9994%. Losses of $(0.45 \pm 0.03) \times 10^{-4}$ for SiO_2 [41] and $(3.6 \pm 0.1) \times 10^{-4}$ for Ta_2O_5 [42] were used for calculations of CTN. The x axis shows only absorption originating from aSi and is therefore at 0 ppm for no aSi layers.

For all coatings, the thermal noise reduction converges to a constant level for absorptions of $\gtrsim 5$ ppm. The reason is that for all coating designs we aimed for a reflectivity of $R = 99.9994\%$. As the sum of absorption, transmission and reflection is defined as 100%, above a certain absorption level, we cannot remove further bilayers of $\text{SiO}_2/\text{Ta}_2\text{O}_5$ or the reflectivity would decrease. The largest error in k was estimated to be $\sim 10\%$ dominated by the measurement reproducibility [35], which directly applies to the x values in Fig. 2. Error bars were omitted for better legibility.

There has been evidence that the total thermal noise of a multilayer coating can be underestimated by extrapolating from single-layer losses. However, here we do not present any thermal noise numbers, but just relative improvements between coating designs which were all calculated based on the same assumptions [41].

An error in mechanical loss affects both the multi-material and the $\text{SiO}_2/\text{Ta}_2\text{O}_5$ coating and, due to the high loss of Ta_2O_5 dominating the coating loss, largely cancels out when looking at the relative CTN improvement (y axis). For the coating with the most Ta_2O_5 replaced with aSi, the relative CTN would change by $< 1\%$ for an error of $\leq 10\%$ for the mechanical losses of all three materials (and less for the other coatings).

1. ATF

The first green diamond, at a coating thermal noise level of 94% and an absorption of 0.07 ppm, represents a coating with one Ta_2O_5 layer at the bottom replaced by one layer of aSi from ATF and some $\text{SiO}_2/\text{Ta}_2\text{O}_5$ removed at the top to keep the reflectivity constant, as described in Sec. IV A and shown in Fig. 1(b).

For the second diamond, the second Ta_2O_5 layer from the bottom was replaced by aSi. One full bilayer of $\text{SiO}_2/\text{Ta}_2\text{O}_5$ plus the “modified” (0.4/1.6) bilayer from the first replacement step were removed at the top, reducing coating thermal noise to 87%. As we move along the dashed line, each diamond represents a coating in which one more Ta_2O_5 layer is replaced with aSi. A maximum coating thermal-noise reduction of about 22% can be achieved with aSi from ATF before the absorption would become too high for a reflectivity of 99.9994% to be realized. The dashed line is used to indicate that not only full layers of Ta_2O_5 can be replaced but also fractions of layers. However, the replacement of fractions does not have a unique solution as we will explain in Sec. VI. Therefore, the dashed lines are only a guide to the eye and partial-layer solutions will not all be positioned exactly on this line.

2. MLD

The MLD coating, represented by the yellow dots and dashed line (top), shows slightly less thermal noise improvement than the ATF coating. While the mechanical loss is assumed to be identical to ATF, the lower refractive index results in thicker aSi layers and in a slightly lower coating reflectivity, which allows for fewer $\text{SiO}_2/\text{Ta}_2\text{O}_5$ bilayers to be removed at the top of the coating. This results in less coating thermal noise reduction compared to the coating using aSi from ATF. The optical absorption is shifted to lower numbers compared to the ATF coating despite the higher k . This is due to more $\text{SiO}_2/\text{Ta}_2\text{O}_5$ layers remaining on top, which reflect more of the light before it reaches the aSi. With aSi from MLD, a maximum coating thermal-noise reduction of 19% can be achieved.

3. Tafelmaier

For the Tafelmaier aSi, both the mechanical loss and the absorption are lower, while the refractive index is higher than for ATF and MLD. Therefore, we win directly in thermal noise from the lower mechanical loss and from the thinner layers reducing d in Eq. (1). Also due to the higher refractive index, fewer $\text{SiO}_2/\text{Ta}_2\text{O}_5$ layers are required to achieve the design reflectivity, further reducing d . This moves the Tafelmaier results, shown by the blue circles, downwards, while the lower absorption moves the points to the left. When only one Ta_2O_5 layer is replaced by aSi, a significant thermal noise improvement of $\approx 15\%$ can be achieved for an absorption increase of 0.2 ppm. A maximum reduction in coating thermal noise of 28% would be

possible for a coating with the required reflectivity of 99.9994%.

4. UWS

aSi made by UWS shows an optical absorption about 1 order of magnitude lower than that of the Tafelmaier coatings. Consequently, coating thermal noise can be improved by almost 30% before the absorption becomes significant. For an absorption of ≈ 3.5 ppm, coating thermal noise reduces by 42% compared to the $\text{SiO}_2/\text{Ta}_2\text{O}_5$ coating shown in Fig. 1(a). For this coating, marked with the dashed circle, only 4.5 bilayers of $\text{SiO}_2/\text{Ta}_2\text{O}_5$ remain on top of 6 bilayers of aSi/SiO₂, see Fig. 3(a).

V. ETM AND ITM

So far we have considered highly reflective coatings suitable for use as the end test-masses (ETMs) in a gravitational-wave detector arm cavity. In the example of Advanced LIGO, the ETM has a reflectivity of 99.9994% [as shown in Fig. 2(a)]. The arm cavity input mirror

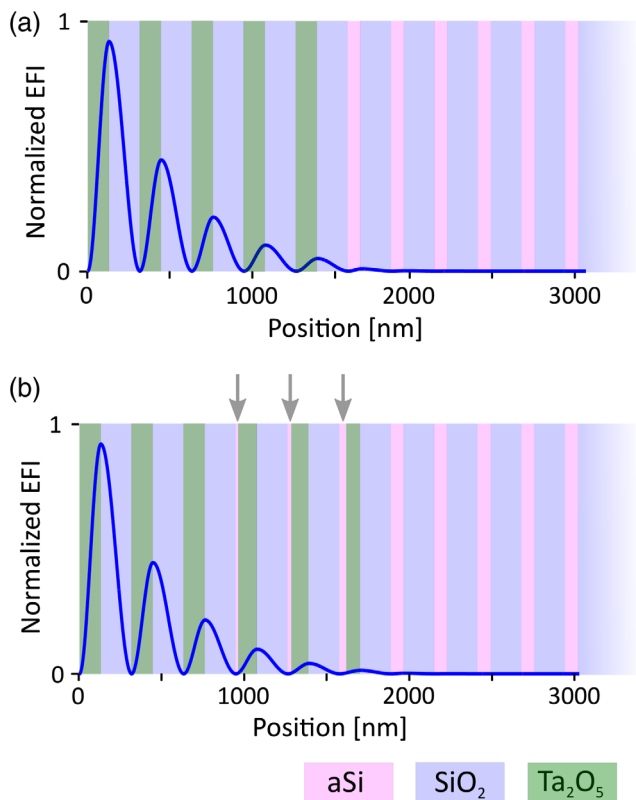


FIG. 3. (a) Schematic of a multilayer coating using aSi from UWS. The absorption and coating thermal noise of this coating are represented by the orange point surrounded by the dotted circle in Fig. 2(a). (b) Coating with a reflectivity identical to that in (a), but with one aSi layer split and forming “mixed” layers with Ta_2O_5 . The mixed layers are marked with arrows. As the EFI in the aSi part of the layers is low, the absorption reduces compared to (a).

[input test mass (ITM)] is lower in reflectivity, $R \approx 98.6\%$ in aLIGO. This reflectivity can be achieved using only 6.5 bilayers (if made of ideal quarter layers) of $\text{SiO}_2/\text{Ta}_2\text{O}_5$ plus an additional bilayer made of 1.65 quarter layers of SiO_2 and 0.35 quarter layers of Ta_2O_5 .⁴

The coating thermal noise of the arm cavity is given by the quadrature sum of the contributions from the ITM and the ETM. Figure 2(b) shows the total thermal noise improvement of the detector, where the ETMs are improved as in Fig. 2(a), and the ITM design (and thermal noise) remains constant, with no aSi layers used.

All coatings using aSi made by MLD, ATF, or Tafelmaier, shown in Fig. 2(a), require 7.5 or more bilayers of $\text{SiO}_2/\text{Ta}_2\text{O}_5$ to reduce the EFI before aSi can be used. Therefore, the ITM cannot benefit by using aSi by any of these vendors. However, the optical absorption of aSi made by UWS is low enough to allow one bilayer of aSi/SiO₂ to be used underneath 4.5 bilayers of $\text{SiO}_2/\text{Ta}_2\text{O}_5$, resulting in the ITM design reflectivity of 98.6% with an absorption of 3.5 ppm. The thermal noise of this coating would be 18% below that of an ITM made of $\text{SiO}_2/\text{Ta}_2\text{O}_5$ only. As fewer Ta_2O_5 layers get replaced, less thermal noise improvement is possible than for the ETM.

If we combine this improved ITM with the UWS ETM of identical absorption, the total thermal noise improvement of the detector would be 33%. This improvement is shown by the orange point labeled “+ITM” in Fig. 2(b).

VI. ABSORPTION OPTIMIZATION

Further improvement is possible by moving the aSi to positions where the EFI is low. Figure 3(a) shows a multilayer coating using aSi from UWS with an absorption of about 3.5 ppm. In the coating shown in Fig. 3(b), the same amount of aSi is used as in (a). However, in (b), the outermost aSi layer was split into 0.5, 0.3, and 0.2 quarter layers (adding up to one quarter layer). Together with fractions of Ta_2O_5 quarter layers, they form some of the high refractive-index layers of the coating—marked with grey arrows. The reflectivity of the coating shown in (b) is identical to that in (a), but its absorption has reduced from 3.5 to 1.8 ppm as the aSi layer fractions are positioned where the light field is low.

The total optical layer thickness of the mixed layers is slightly larger than a quarter of a wavelength to keep the reflection maximum and the absorption minimum at the design wavelength, resulting in ≈ 2.34 instead of 2 layers of Ta_2O_5 . Consequently, coating (b) has slightly higher coating thermal noise than coating (a) with an overall reduction of 40.5% (instead of 42%) compared to a $\text{SiO}_2/\text{Ta}_2\text{O}_5$ coating.

The upper, gray square in Fig. 2(b) shows the detector coating thermal noise when the optimized coating is

⁴Note that this is a simplified example and not the actual design of the Advanced LIGO ITMs.

combined with a classical ITM (without aSi). For the bottom, gray square, the ITM was also optimized.⁵ When using mixed layers in both the ITM and ETM, a coating thermal noise improvement of 28.5% is possible at an absorption of about 1.8 ppm per mirror (compared to 32% for about 3.5 ppm).

This is an example to illustrate the concept, which we tried to keep as simple as possible while keeping the layers realistically thick (from a deposition perspective). Some other options for incorporating aSi into multimaterial coatings via stacked-triplet design have recently been investigated by Pinto [43].

VII. REFLECTIVITY OF GREEN LIGHT

A way to stabilize the detectors' arm length is the use of 532 nm laser light [44,45]. All coating designs discussed so far were optimized for high reflectivity at 1064 nm only. If, for example, the layer thicknesses of the coating shown in Fig. 3(a) were adjusted to 1.27 quarter layers for the low, and to 0.71 quarter layers for the high-index layers, a reflectivity of $\approx 96\%$ at 532 nm could be achieved. To maintain the reflectivity at 1064 nm at 99.9994%, in this example, two bilayers of aSi/SiO₂ would have to be added at the bottom of the coating.

The additional CTN from these two additional bilayers is low due to the low mechanical loss of these materials. Furthermore, the thickness of the high-loss Ta₂O₅ layers is reduced and the peak EFI is moved from the layer interfaces into the low-loss SiO₂ layers, reducing the overall CTN. This type of design for reflectivity at two wavelengths is very similar to that previously suggested for CTN optimization [46,47], as Eq. (1) shows.

In reality, the Advanced LIGO coatings have an optimized design to enable high reflectivity at both 532 nm and 1064 nm, which also results in a slight CTN reduction. Here, for simplicity, we do not consider thickness optimization for 532 nm reflectivity. However, when optimizing both our reference SiO₂/Ta₂O₅ coating and our multimaterial coating, to first order any CTN improvement would be likely to cancel out, as we only consider the relative improvement between coatings.

While from the reflectance perspective there are no objections to this, the optical absorption of aSi at 532 nm is known to be high. For the UWS coatings, we do not have absorption data at this wavelength, but for the Tafelmaier coatings, a k of about 0.8 was found, which is in agreement with literature⁶ and which we will assume here as an upper bound for the UWS aSi. At this level of

absorption, all 532 nm light transmitted into the aSi layers would be absorbed. Therefore, it would not be possible to inject the 532 nm light into the interferometer through the ETMs, but another solution would have to be found, e.g., coupling the green light in through (aSi-free) ITMs as in KAGRA [48].

VIII. CONCLUSION

We have shown that coating thermal noise in gravitational-wave detectors operating at 1064 nm and at room temperatures could be improved by using aSi in a multimaterial coating design. The achievable improvement is a trade-off between thermal noise reduction and absorption increase.

With state-of-the-art commercial coatings, only the ETMs could be improved, while with material in the development phase, an improvement of the ITM would also be possible. By splitting some high-index layers into "mixed" layers made of aSi and Ta₂O₅, the absorption can additionally be reduced. For the best aSi identified so far, a thermal noise reduction of almost 30% in the detectors would be possible for an optical absorption of about 1.8 ppm per mirror due to the aSi. (For a higher tolerable absorption, more improvement is possible, for a lower tolerable absorption, it is less.) This approach may therefore be an attractive option.

While the absorption of 532 nm laser light in the aSi layers should not impose a major problem on the coating reflectivity, injecting 532 nm light through the ETMs would very likely not be possible and would need a different solution.

The aSi-based multimaterial coating design is versatile and can easily be used in conjunction with other developments—for example, by replacing the remaining Ta₂O₅ by a material with lower mechanical loss. Several such materials are currently under development in the community, and we believe that combining these new materials with our multimaterial approach has excellent potential to fully meet the requirements of future room-temperature GW detectors.

ACKNOWLEDGMENTS

We are grateful for financial support from STFC (ST/N005422/1), the Royal Society (RG110331), and the University of Glasgow. We acknowledge support from the International Max Planck Partnership for Measurement and Observation at the Quantum Limit and from Interreg Euregio Meuse Rhine (E-TEST project). I. W. M. was supported by a Royal Society Research Fellowship while working on this paper. We would like to thank I. Jones for helping to make the obvious invisible, and our colleagues in the LSC and Virgo Collaborations, in particular I. Pinto, and within SUPA for their interest in this work. This paper has LIGO Document No. LIGO-P2000333.

⁵From the top two bilayers of SiO₂/Ta₂O₅, (0.2 × aSi + 0.9 × Ta₂O₅)/SiO₂, (0.3 × aSi + 0.8 × Ta₂O₅)/SiO₂, (0.4 × aSi + 0.7 × Ta₂O₅)/SiO₂, Ta₂O₅.

⁶refractiveindex.info

- [1] B. P. Abbott, R. Abbott, T. D. Abbott, M. R. Abernathy, F. Acernese, K. Ackley, C. Adams, T. Adams, P. Addesso, R. X. Adhikari *et al.* (LIGO Scientific Collaboration and Virgo Collaboration), GW150914: The Advanced LIGO Detectors in the Era of First Discoveries, *Phys. Rev. Lett.* **116**, 131103 (2016).
- [2] F. Acernese *et al.*, Advanced Virgo: A second-generation interferometric gravitational wave detector, *Classical Quantum Gravity* **32**, 024001 (2015).
- [3] B. P. Abbott, R. Abbott, T. D. Abbott, M. R. Abernathy, F. Acernese, K. Ackley, C. Adams, T. Adams, P. Addesso, R. X. Adhikari *et al.* (LIGO Scientific Collaboration and Virgo Collaboration), Observation of Gravitational Waves from a Binary Black Hole Merger, *Phys. Rev. Lett.* **116**, 061102 (2016).
- [4] B. P. Abbott, R. Abbott, T. D. Abbott, M. R. Abernathy, F. Acernese, K. Ackley, C. Adams, T. Adams, P. Addesso, R. X. Adhikari *et al.* (LIGO Scientific Collaboration and Virgo Collaboration), GW151226: Observation of Gravitational Waves from a 22-Solar-Mass Binary Black Hole Coalescence, *Phys. Rev. Lett.* **116**, 241103 (2016).
- [5] B. P. Abbott, R. Abbott, T. D. Abbott, F. Acernese, K. Ackley, C. Adams, T. Adams, P. Addesso, R. X. Adhikari, and V. B. Adya (LIGO Scientific Collaboration and Virgo Collaboration), GW170104: Observation of a 50-Solar-Mass Binary Black Hole Coalescence at Redshift 0.2, *Phys. Rev. Lett.* **118**, 221101 (2017).
- [6] B. P. Abbott, R. Abbott, T. D. Abbott, F. Acernese, K. Ackley, C. Adams, T. Adams, P. Addesso, R. X. Adhikari, and V. B. Adya (LIGO Scientific Collaboration and Virgo Collaboration), GW170814: A Three-Detector Observation of Gravitational Waves from a Binary Black Hole Coalescence, *Phys. Rev. Lett.* **119**, 141101 (2017).
- [7] B. P. Abbott, R. Abbott, T. D. Abbott, M. R. Abernathy, F. Acernese, K. Ackley, C. Adams, T. Adams, P. Addesso, R. X. Adhikari *et al.* (LIGO Scientific Collaboration and Virgo Collaboration), GWTC-1: A Gravitational-Wave Transient Catalog of Compact Binary Mergers Observed by LIGO and Virgo During the First and Second Observing Runs, *Phys. Rev. X* **9**, 031040 (2019).
- [8] B. P. Abbott, R. Abbott, T. D. Abbott, F. Acernese, K. Ackley, C. Adams, T. Adams, P. Addesso, R. X. Adhikari, V. B. Adya *et al.* (LIGO Scientific Collaboration and Virgo Collaboration), GW170817: Observation of Gravitational Waves from a Binary Neutron Star Inspiral, *Phys. Rev. Lett.* **119**, 161101 (2017).
- [9] G. M. Harry, H. Armandula, E. Black, D. R. M. Crooks, G. Cagnoli, J. Hough, P. Murray, S. Reid, S. Rowan, P. Sneddon, M. M. Fejer, R. Route, and S. D. Penn, Thermal noise from optical coatings in gravitational wave detectors, *Appl. Opt.* **45**, 1569 (2006).
- [10] G. M. Harry *et al.*, Titania-doped tantala/silica coatings for gravitational-wave detection, *Classical Quantum Gravity* **24**, 405 (2007).
- [11] R. Flaminio, J. Franc, C. Michel, N. Morgado, L. Pinard, and B. Sassolas, A study of coating mechanical and optical losses in view of reducing mirror thermal noise in gravitational wave detectors, *Classical Quantum Gravity* **27**, 084030 (2010).
- [12] M. Granata, E. Saracco, N. Morgado, A. Cajgfinger, G. Cagnoli, J. Degallaix, V. Dolique, D. Forest, J. Franc, C. Michel, L. Pinard, and R. Flaminio, Mechanical loss in state-of-the-art amorphous optical coatings, *Phys. Rev. D* **93**, 012007 (2016).
- [13] M. Granata, A. Amato, L. Balzarini, M. Canepa, J. Degallaix, D. Forest, V. Dolique, L. Mereni, C. Michel, L. Pinard, B. Sassolas, J. Teillon, and G. Cagnoli, Amorphous optical coatings of present gravitational-wave interferometers, *Classical Quantum Gravity* **37**, 095004 (2020).
- [14] M. J. Hart, R. Bassiri, K. B. Borisenko, M. Véron, E. F. Rauch, I. W. Martin, S. Rowan, M. M. Fejer, and I. MacLaren, Medium range structural order in amorphous tantala spatially resolved with changes to atomic structure by thermal annealing, *J. Non-Cryst. Solids* **438**, 10 (2016).
- [15] J. P. Trinastic, R. Hamdan, C. Billman, and H.-P. Cheng, Molecular dynamics modeling of mechanical loss in amorphous tantala and titania-doped tantala, *Phys. Rev. B* **93**, 014105 (2016).
- [16] R. Bassiri, M. R. Abernathy, F. Liou, A. Mehta, E. K. Gustafson, M. J. Hart, H. N. Isa, N. Kim, A. C. Lin, I. MacLaren, I. W. Martin, R. K. Route, S. Rowan, B. Shyam, J. F. Stebbins, and M. M. Fejer, Order, disorder and mixing: The atomic structure of amorphous mixtures of titania and tantala, *J. Non-Cryst. Solids* **438**, 59 (2016).
- [17] G. Vajente *et al.*, Effect of elevated substrate temperature deposition on the mechanical losses in tantala thin film coatings, *Classical Quantum Gravity* **35**, 075001 (2018).
- [18] L. Pinard, C. Michel, B. Sassolas, L. Balzarini, J. Degallaix, V. Dolique, R. Flaminio, D. Forest, M. Granata, B. Lagrange, N. Straniero, J. Teillon, and G. Cagnoli, Mirrors used in the LIGO interferometers for first detection of gravitational waves, *Appl. Opt.* **56**, C11 (2017).
- [19] H.-W. Pan, L.-C. Kuo, L.-A. Chang, S. Chao, I. W. Martin, J. Steinlechner, and M. Fletcher, Silicon nitride and silica quarter-wave stacks for low-thermal-noise mirror coatings, *Phys. Rev. D* **98**, 102001 (2018).
- [20] K. Craig, J. Steinlechner, P. Murray, R. B. A. Bell, K. Haughian, J. Hough, I. MacLaren, S. Penn, S. Reid, R. Robie, S. Rowan, and I. W. Martin, Mirror Coating Solution for the Cryogenic Einstein Telescope, *Phys. Rev. Lett.* **122**, 231102 (2019).
- [21] A. Amato, G. Cagnoli, M. Canepa, E. Coillet, J. Degallaix, V. Dolique, D. Forest, M. Granata, V. Martinez, C. Michel, L. Pinard, B. Sassolas, and J. Teillon, High-reflection coatings for gravitational-wave detectors: State of the art and future developments, *J. Phys. Conf. Ser.* **957**, 012006 (2018).
- [22] H.-W. Pan, S.-J. Wang, L.-C. Kuo, S. Chao, M. Principe, I. M. Pinto, and R. DeSalvo, Thickness-dependent crystallization on thermal anneal for titania/silica nm-layer composites deposited by ion beam sputter method, *Opt. Express* **22**, 29847 (2014).
- [23] R. Birney, J. Steinlechner, Z. Tomasi, S. MacFoy, D. Vine, A. S. Bell, D. Gibson, J. Hough, S. Rowan, P. Sortais, S. Sproules, S. Tait, I. W. Martin, and S. Reid, Amorphous Silicon with Extremely Low Absorption: Beating Thermal Noise in Gravitational Astronomy, *Phys. Rev. Lett.* **121**, 191101 (2018).

- [24] G. D. Cole, W. Zhang, B. J. Bjork, D. Follman, P. Heu, C. Deutsch, L. Sonderhouse, J. Robinson, C. Franz, A. Alexandrovski, M. Notcutt, O. H. Heckl, J. Ye, and M. Aspelmeyer, High-performance near- and mid-infrared crystalline coatings, *Optica* **3**, 647 (2016).
- [25] X. Liu, B. E. White, Jr., R. O. Pohl, E. Iwanizcko, K. M. Jones, A. H. Mahan, B. N. Nelson, R. S. Crandall, and S. Veprek, Amorphous Solid Without Low Energy Excitations, *Phys. Rev. Lett.* **78**, 4418 (1997).
- [26] I. H. Malitson, Interspecimen comparison of the refractive index of fused silica, *J. Opt. Soc. Am.* **55**, 1205 (1965).
- [27] A. Amato, S. Terreni, V. Dolique, D. Forest, G. Gemme, M. Granata, L. Mereni, C. Michel, L. Pinard, B. Sassolas, J. Teillon, G. Cagnoli, and M. Canepa, Optical properties of high-quality oxide coating materials used in gravitational-wave advanced detectors, *J. Phys. Mater.* **2**, 035004 (2019).
- [28] J. Steinlechner, I. W. Martin, R. Bassiri, A. Bell, M. M. Fejer, J. Hough, A. Markosyan, R. K. Route, S. Rowan, and Z. Tornasi, Optical absorption of ion-beam sputtered amorphous silicon coatings, *Phys. Rev. D* **93**, 062005 (2016).
- [29] J. Steinlechner, I. W. Martin, J. Hough, C. Krueger, S. Rowan, and R. Schnabel, Thermal noise reduction and absorption optimization via multimaterial coatings, *Phys. Rev. D* **91**, 042001 (2015).
- [30] W. Yam, S. Gras, and M. Evans, Multimaterial coatings with reduced thermal noise, *Phys. Rev. D* **91**, 042002 (2015).
- [31] S. C. Tait, J. Steinlechner, M. M. Kinley-Hanlon, P. G. Murray, J. Hough, G. McGhee, F. Pein, S. Rowan, R. Schnabel, C. Smith, L. Terkowski, and I. W. Martin, Demonstration of the Multimaterial Coating Concept to Reduce Thermal Noise in Gravitational-Wave Detectors, *Phys. Rev. Lett.* **125**, 011102 (2020).
- [32] T. Hong, H. Yang, E. K. Gustafson, R. X. Adhikari, and Y. Chen, Brownian thermal noise in multilayer coated mirrors, *Phys. Rev. D* **87**, 082001 (2013).
- [33] G. M. Harry, A. M. Gretarsson, P. R. Saulson, S. E. Kittelberger, S. D. Penn, W. J. Startin, S. Rowan, M. M. Fejer, D. R. M. Crooks, G. Cagnoli, J. Hough, and N. Nakagawa, Thermal noise in interferometric gravitational wave detectors due to dielectric optical coatings, *Classical Quantum Gravity* **19**, 897 (2002).
- [34] M. A. Green and M. J. Keever, Optical properties of intrinsic silicon at 300 k, *Prog. Photovoltaics Res. Appl.* **3**, 189 (1995).
- [35] J. Steinlechner, Absorption of asi at 1064 nm, LIGO document No. T2000481, 2020.
- [36] M. R. Abernathy, Mechanical properties of coating materials for use in the mirrors of interferometric gravitational wave detectors, Ph.D. Thesis, University of Glasgow, 2012.
- [37] P. G. Murray, I. W. Martin, K. Craig, J. Hough, R. Robie, S. Rowan, M. R. Abernathy, T. Pershing, and S. Penn, Ion-beam sputtered amorphous silicon films for cryogenic precision measurement systems, *Phys. Rev. D* **92**, 062001 (2015).
- [38] J. Steinlechner, I. W. Martin, A. S. Bell, J. Hough, M. Fletcher, P. G. Murray, R. Robie, S. Rowan, and R. Schnabel, Silicon-Based Optical Mirror Coatings for Ultra-high Precision Metrology and Sensing, *Phys. Rev. Lett.* **120**, 263602 (2018).
- [39] A. F. Brooks *et al.*, Overview of advanced LIGO adaptive optics, *Appl. Opt.* **55**, 8256 (2016).
- [40] L. Pinard, C. Michel, B. Sassolas, L. Balzarini, J. Degallaix, V. Dolique, R. Flaminio, D. Forest, M. Granata, B. Lagrange, N. Straniero, J. Teillon, and G. Cagnoli, Mirrors used in the LIGO interferometers for first detection of gravitational waves, *Appl. Opt.* **56**, C11 (2017).
- [41] M. Granata, E. Saracco, N. Morgado, A. Cajgfinger, G. Cagnoli, J. Degallaix, V. Dolique, D. Forest, J. Franc, C. Michel, L. Pinard, and R. Flaminio, Mechanical loss in state-of-the-art amorphous optical coatings, *Phys. Rev. D* **93**, 012007 (2016).
- [42] S. Gras and M. Evans, Direct measurement of coating thermal noise in optical resonators, *Phys. Rev. D* **98**, 122001 (2018).
- [43] I. Pinto, Ternary quarter wavelength coatings for gravitational wave detector mirrors: Design optimization via exhaustive search, [arXiv:2012.02146](https://arxiv.org/abs/2012.02146).
- [44] J. Aasi, B. P. Abbott, R. Abbott, T. Abbott, M. R. Abernathy, K. Ackley, C. Adams, T. Adams, P. Addesso, R. X. Adhikari *et al.*, Advanced LIGO, *Classical Quantum Gravity* **32**, 074001 (2015).
- [45] A. J. Mullavey, B. J. J. Slagmolen, J. Miller, M. Evans, P. Fritschel, D. Sigg, S. J. Waldman, D. A. Shaddock, and D. E. McClelland, Arm-length stabilisation for interferometric gravitational-wave detectors using frequency-doubled auxiliary lasers, *Opt. Express* **20**, 81 (2012).
- [46] A. E. Villar, E. D. Black, R. DeSalvo, K. G. Libbrecht, C. Michel, N. Morgado, L. Pinard, I. M. Pinto, V. Pierro, V. Galdi, M. Principe, and I. Taurasi, Measurement of thermal noise in multilayer coatings with optimized layer thickness, *Phys. Rev. D* **81**, 122001 (2010).
- [47] M. Principe, Reflective coating optimization for interferometric detectors of gravitational waves, *Opt. Express* **23**, 10938 (2015).
- [48] T. Akutsu, M. Ando, K. Arai, K. Arai, Y. Arai, S. Araki, A. Araya, N. Aritomi, Y. Aso, S. Bae *et al.*, An arm length stabilization system for KAGRA and future gravitational-wave detectors, *Classical Quantum Gravity* **37**, 035004 (2020).